Vapor-Deposited Emittance-Catalysis Coatings for Superalloys in Heat-Shield Applications

Ronald K. Clark*
NASA Langley Research Center, Hampton, Virginia
and
George R. Cunnington Jr.† and John C. Robinson ‡
Lockheed Palo Alto Research Laboratory, Palo Alto, California

Results are presented for dynamic oxidation tests of Inconel 617 and MA 956 superalloy specimens prepared with aluminosilicate coatings formulated to have a high emittance and a low catalytic activity. Results indicate that coated MA 956 has a much lower catalytic activity after 5½ h (19 cycles to temperature) of exposure at temperatures near 1370 K than does uncoated MA 956. The net effect of emittance-catalysis enhancement coatings on MA 956 is a 100% increase in the energy input required to produce a surface temperature of 1370 K. The net effect of the coating on Inconel 617 is a 50% increase in the energy input required to produce the same surface temperature. This lesser effect for Inconel 617 results from interaction between the coating and the oxides of the Inconel 617 alloy.

Nomenclature

H_{cw}, H_w = total enthalpy of equilibrium air at ambient and wall temperatures, respectively, J/kg
H_{e0} = total boundary layer edge enthalpy at the stagnation point, J/kg
P = model stagnation pressure, Pa
$\dot{q}_{CCW}, \dot{q}_{CHW}$ = catalytic cold and hot wall heating rate, respectively, W/m^2
$\dot{q}_{COND}$ = conduction heat loss from the specimen, W/m^2
R_B, R_{eff} = radius and effective radius of model, respectively, m
T = surface temperature, K
ϵ_{TH} = total hemispherical emittance of the surface
σ = Stephan-Boltzman constant (5.67×10^{-8} W/m^{2}K^4)

Introduction

TWO alloys of potential interest for Thermal Protection System (TPS) applications are Inconel 617 and MA 956. Inconel 617, a nickel-chromium superalloy, has been shown to meet the high-temperature strength, oxidation resistance, and high emittance criteria for use in TPS applications.[1-3] MA 956, an oxide-dispersion-strengthened iron-base superalloy, also has good high-temperature strength and very good oxidation resistance,[4] but it has a relatively low emittance.

In addition to strength, oxidation resistance, and emittance, a parameter of major importance in considering materials for TPS applications is the catalytic activity of the surface to recombination of dissociated oxygen and nitrogen, which are present at significant levels in the boundary layer of entry vehicles during peak heating for Space Shuttle-like trajectories. Surface catalysis experiments on Space Shuttle flights STS-2 through STS-5 showed that high surface catalytic activity can result in surface temperatures along the lower centerline of the vehicle that are 110 to 275 K higher than those of the high-temperature reuseable-surface insulation tiles used on the current Space Shuttle.[5]

The purpose of this research was to investigate the feasibility of using vapor-deposited coatings to increase the emittance and decrease the catalytic activity of superalloys exposed to dynamic oxidation conditions representative of a re-entry environment. Statically oxidized specimens of Inconel 617 and MA 956 superalloys were prepared with micrometer-thick layers of aluminosilicate coatings. Specimens were exposed to dynamic oxidation conditions followed by radiative and metallurgical analyses.

Experimental Procedure

Test Specimens

Test specimens (2.5-cm-diam disks) of Inconel 617 and MA 956 were stamped from commercially available sheet material of 0.8- and 0.3-mm thickness, respectively. Table 1 gives the chemical analysis of both alloys as provided by the vendor.

The specimens were prepared for coating with a thorough cleaning. The Inconel 617 specimens were then oxidized in static air at 1255 K for 10 h; the MA 956 specimens were lightly grit-blasted with 120-mesh alumina followed by static oxidation at 1370 K for 2 h. The oxidized Inconel 617 specimens were coated with a layer of evaporated aluminum approximately 1 μm thick.

The coatings (developed by Lockheed Missiles and Space Company) were deposited directly onto the MA 956 superalloy and onto the aluminum layer previously evaporated onto the Inconel 617 superalloy using a chemical vapor deposition process. The specimens were subsequently heat-treated in air to oxidize the layer and complete the reactions within the coating. This resulted in the formation of a layer of an aluminosilicate-type composition on the order of 1 μm thick in both cases.

Exposure of Specimens

Selected specimens were exposed to a series of short-duration tests (1 to 3 min) at different conditions to provide heating rate/temperature data for comparison of coated and uncoated specimens of both alloys. To test the longer-term performance of the coatings, specimens were exposed to cyclic

Presented as Paper 85-403 at the AIAA 23rd Aerospace Sciences Meeting, Reno, NV, Jan. 14-17, 1985; received April 11, 1985; revision received Jan. 23, 1986.

*Research Scientist, Materials Division. Member AIAA.
†Senior Member of Research Laboratory. Member AIAA.
‡Staff Scientist.

tests of about ½ h each at constant temperatures for total exposure times of up to 8 hs.

Specimens were exposed to dynamic oxidation conditions at surface temperatures ranging from 1090 to 1480 K in the Langley Research Center Hypersonic Materials Environmental Test System (HYMETS), which is a 100-kW constrictor-arc-heated wind tunnel.[6] The range of aerothermal heating conditions utilized is given in Table 2. The test conditions did not provide for full simulation of any current or projected re-entry environment. The heat flux—the most critical response parameter—was representative of the levels encountered during peak heating for Space Shuttle-like trajectories. The surface pressure and freestream enthalpy were one-half to one-fourth the levels expected during such trajectories. The surface temperature of specimens during simulated re-entry testing was monitored using a narrow-band radiation pyrometer with emittance correction.

Table 3 gives the nominal flowfield composition for two enthalpy levels. The data are based upon boundary layer edge conditions calculated using the Aerotherm Chemical Equilibrium (ACE) code.[7] The data indicate that oxygen in the test stream is nearly completely dissociated, whereas nitrogen is only partially dissociated even at the higher enthalpy level.

Materials Analysis Techniques

Assessment of Catalytic Activity

A direct assessment of the catalytic activity of TPS materials under dynamic oxidation conditions cannot be made. Two indirect means that may be utilized to qualitatively judge the catalytic activity of materials are 1) comparison of heating rates and equilibrium surface temperatures for different materials and 2) comparison of the surface catalysis ratios for different materials. The basis for these comparisons is the fact that the heating rate to a catalytic surface in a given environment consists of a convective component and a catalytic component (which results from recombination of dissociated species). The heating rate to the surface of a material with a low catalytic activity will include only a portion of the available energy due to recombination reactions.

For the present study the surface catalysis ratio was defined as the ratio of the net aerothermal heating rate, expressed as the sum of the surface-equilibrium-radiative heat loss and conduction loss, and the catalytic hot-wall heating rate.[8] It was calculated using

$$\text{Surface catalysis ratio} = [\sigma \epsilon_{TH} T^4 + \dot{q}_{COND}]/\dot{q}_{CHW} \quad (1)$$

where ϵ_{TH} was obtained by correlation from the measured total normal emittance values, $\dot{q}_{COND}$ was obtained from transient cooling data from a thermocouple attached to the specimen, and $\dot{q}_{CHW}$ was calculated using

$$\dot{q}_{CHW} = \dot{q}_{CCW} \frac{H_{e0} - H_w}{H_{e0} - H_{cw}} \quad (2)$$

The catalytic cold-wall heating rate for a stagnation point model[9] is given by

$$\dot{q}_{CCW} = 3.60 \times 10^{-4} (H_{eo} - H_w) \sqrt{\frac{P}{R_{eff}}} \quad (3)$$

where $R_{eff} = 3.78\ R_B$ for a flat-face model at low Mach numbers.[8] For the 15.9-mm-radius flat-face model utilized herein, Eq. (3) was rearranged to obtain an approximate expression for the total enthalpy of the flowfield,

$$H_{e0} = 690 \frac{\dot{q}_{CCW}}{\sqrt{P}} + H_w \quad (4)$$

Analysis of Oxidation

Mass changes of specimens were determined by weighing them before and after exposure to dynamic oxidation conditions. These data were normalized by the total surface area to obtain weight change per area. The mass change data for coated specimens were used as a qualitative indicator of coating stability under test conditions.

The morphologies of specimen oxides were studied using conventional light microscopy and Scanning Electron Microscopy (SEM). The oxide-substrate composition was analyzed by Energy Dispersive Analysis of X-Rays (EDAX) and by X-Ray Diffraction analysis (XRD).

EDAX elemental line scans of polished cross sections of specimens were performed to determine the oxide-substrate elemental profiles.

Radiative Property Measurements

Room-temperature spectral near-normal reflectance measurements were made using a Gier-Dunkle HC 300 heated cavity reflectometer and a Cary Model 17 spectrophotometer with integrating sphere attachment. The HC 300 reflectometer was used for the wavelength region from 2 to 24 μm and the Cary spectrophotometer was used for the region of 0.30 to 2.20 μm. The reflectance data were used to find the corresponding values of emittance using the relationships that for opaque surfaces the spectral absorptance is equal to unity minus the spectral reflectance and, by Kirchoff's Law, the spectral emittance is equal to the spectral absorptance at equivalent temperatures. The spectral data were integrated with respect to the Planck blackbody energy distribution curve for temperatures above ambient to arrive at corresponding elevated temperature total normal emittance values.

Table 1 Inconel 617 and MA 956 analyses

Inconel 617		MA 956	
Element	Wt. %	Element	Wt.%
Ni	Balance	Fe	Balance
Cr	22.63	Cr	19.30
Co	12.33	Al	4.28
Mo	9.38	Y	0.49
Al	1.15	Ti	0.39
Fe	0.76	Ni	0.28
Ti	0.27	O	0.20
Si	0.15	Si	0.11
Cu	0.06	Mn	0.09
C	0.05	Co	<0.05
Mn	0.02	N	0.032
S	0.001	C	0.021
		Cu	<0.01
		P	0.009
		S	0.003

Table 2 Range of conditions for dynamic oxidation exposure of superalloys

Specimen surface temperature, K	1145–1480
Surface pressure, Pa	490–815
Free stream Mach number	3.5
Free stream enthalpy, MJ/kg	3.7–10.5
Catalytic hot-wall heating rate, kW/m^2	80–360

Table 3 Nominal test stream composition

	Mole fraction at	
Chemical species	$H_{e0} = 6.6$ MJ/kg	$H_{e0} = 8.4$ MJ/kg
N_2	0.664	0.643
O_2	0.230×10^{-1}	0.604×10^{-3}
N	0.305×10^{-3}	0.112×10^{-1}
O	0.294	0.340
NO	0.182×10^{-1}	0.553×10^{-2}
NO_2	0.270×10^{-6}	0.800×10^{-8}
N_2O	0.839×10^{-7}	0.238×10^{-7}

Results and Discussion

Catalysis Characteristics

Figure 1 shows data for equilibrium surface temperature vs catalytic hot-wall heating rate for short-time dynamic oxidation tests of coated and uncoated Inconel 617 and MA 956 specimens. The figure also shows calculated results for the equilibrium temperature of a fully catalytic surface given by

$$T = \left(\frac{\dot{q}_{CHW} - \dot{q}_{COND}}{\sigma \epsilon_{TH}} \right)^{1/4} \quad (5)$$

The two solid curves are for emittance values of 0.87 and 0.60, which are the nominal emittances of uncoated Inconel 617 and MA 956.

The similarity of calculated results and experimental results for uncoated Inconel 617 and MA 956 indicates that both alloys in the uncoated state tend to be catalytic to the recombination reaction of dissociated species in the dynamic oxidation environment. The measured temperature of uncoated Inconel 617, which was greater than the calculated result, was probably due to error in the emittance correction used on the pyrometer for that specimen.

The experimental data in Fig. 1 form four distinct sets. The difference between the sets resulted from differences in emittance and/or catalytic activity of the specimens. In considering data sets for coated and uncoated specimens of a single alloy that have about the same emittance, the differences between the two sets of data for each alloy were attributed to changes in the specimen catalytic activity the coating caused by. The catalytic activity of the coated MA 956 specimen was so low that it had a lower equilibrium temperature than did the coated Inconel 617 specimen, which had a much higher emittance.

Figure 2 presents surface-catalysis-ratio data as a function of surface temperature for the tests shown in Fig. 1. Again the data are contained within four consistent groups. The surface-catalysis ratios calculated for the uncoated specimens were greater than 1.0 in some instances. This is the result of experimental uncertainties in the measurements of convective heating rate and surface temperature, the accurate knowledge of the total hemispherical emittance of the surface at all times during the exposure to dynamic oxidation conditions, and the calculation of $\dot{q}_{CHW}$ (derived from calculation of H_{e0}). A 2% error in temperature measurement would give an 8% error in surface radiative heat flux. Similarly an error of 3% in the total hemispherical emittance used in calculating the surface radiative heat loss would result in an error of 3% for the Inconel 617 specimens and 4% for the MA 956 specimens. The combination of these two factors gave a maximum uncertainty of 11–12% in the computation of the surface catalysis ratios. The results in Fig. 2 are qualitative only and were interpreted as indicating that uncoated Inconel 617 and MA 956 were catalytic under the dynamic oxidation conditions of the present study. The surface catalysis ratios of coated Inconel 617 and MA 956 were much lower than their uncoated mates; in fact, the surface catalysis ratio of coated MA 956 was about half the surface catalysis ratio of uncoated MA 956.

The variation in catalytic activity with dynamic oxidation time for coated and uncoated Inconel 617 and MA 956 is shown in Fig. 3. The surface catalysis ratio for uncoated MA 956 decreased with time of exposure, reaching a value 70% of its original level after 5½ h. The surface catalysis ratios of coated Inconel 617 and MA 956 were nearly constant with time of exposure.

Oxidation Characterization

Results for weight change with dynamic oxidation exposure time for representative specimens are shown in Fig. 4. The results for coated and uncoated Inconel 617 showed a loss of weight with exposure. The weight loss for coated alloy was generally less than reported for uncoated alloy.[10] The weight

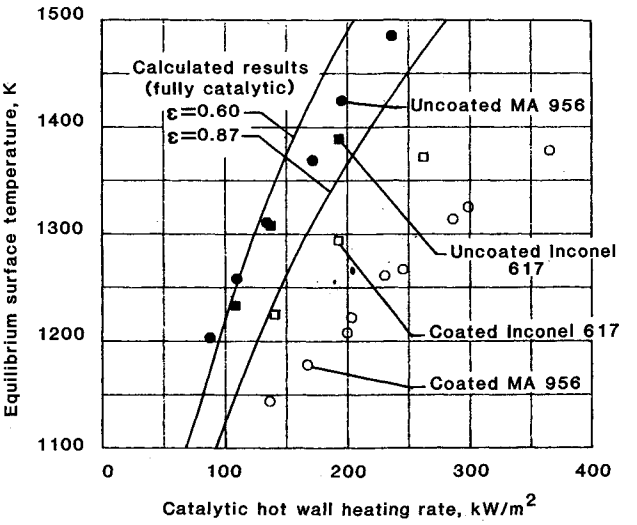

Fig. 1 Equilibrium surface temperature of coated and uncoated superalloys under dynamic oxidation conditions.

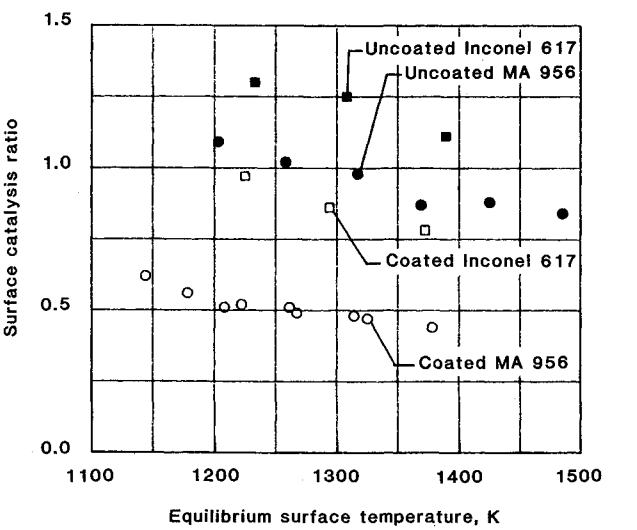

Fig. 2 Surface catalysis ratio versus surface temperature for short-time dynamic oxidation exposure of superalloys.

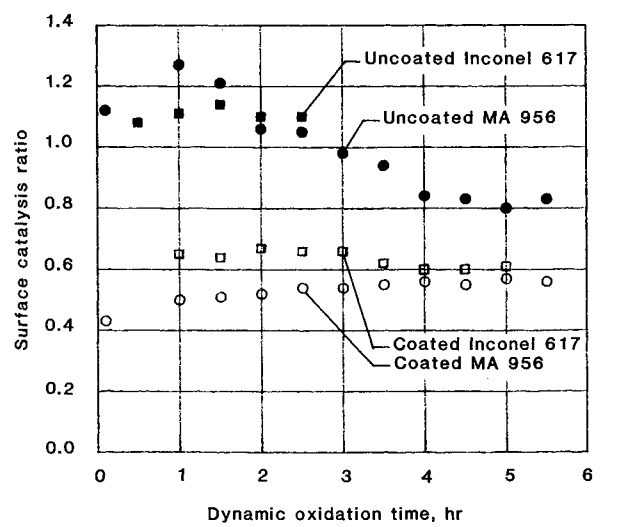

Fig. 3 Variation in surface catalysis ratio of superalloys with exposure to dynamic oxidation conditions.

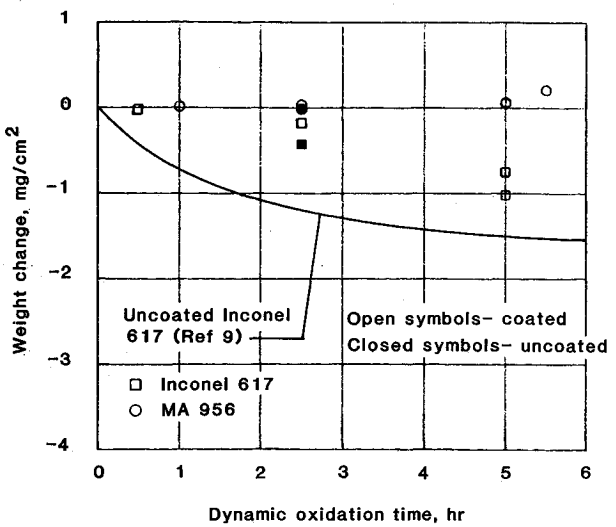

Fig. 4 Weight change of Inconel 617 and MA 956 during exposure to dynamic oxidation conditions.

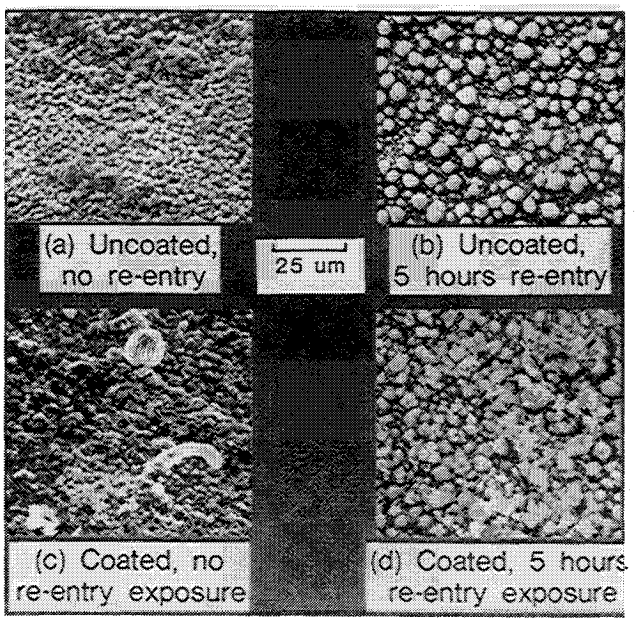

Fig. 5 SEM photographs of Inconel 617 specimens.

of uncoated MA 956 specimens was essentially unchanged by exposure to test conditions.[4] However, the coated MA 956 showed a very small increase in weight with exposure.

Figure 5 shows SEM photographs of the surface oxides of coated and uncoated Inconel 617 specimens before and after exposure to dynamic oxidation conditions. The SEM photograph of the uncoated specimen (a) shows the statically formed oxide that was flat and uniform in topography. The SEM photograph of the uncoated specimen after 2½ h of exposure shows the characteristic spherical oxide particles reported in the literature for superalloys after dynamic oxidation.[10-12] The SEM photograph of the coated specimen after exposure (Fig. 5c) shows evidence of heavy oxidation of the coating, with some evidence of spherical oxide particles of the type shown in Fig. 5b.

Figure 6 shows EDAX line scans of polished cross sections of coated Inconel 617 specimens before and after exposure to dynamic oxidation conditions. The data give a graphic representation of the substrate-oxide-coating system. The very high Cr level at the surface (Fig. 6a) was typical of oxides formed on Inconel 617 in a static air environment. On exposure to dynamic oxidation conditions, the Cr_2P_3 layer formed during static oxidation was quickly removed by oxidizing to form gaseous CrO_3

$$Cr_2O_3 + 3O \rightarrow 2CrO_3 \qquad (6)$$

Removal of the surface layer of Cr_2O_3 leads to accelerated oxidation of the alloy.[11] The presence of the aluminosilicate layer on the coated specimen was evidenced by the strong aluminum and silicon levels at the surface (Fig. 6b). Chromium diffused to the surface and oxidized, resulting in a CR-depleted zone near the substrate-oxide interface. The Cr-depleted zone was more pronounced in the post-exposure specimen than in the specimen with no dynamic oxidation exposure.

Figure 7 shows SEM photographs of the surface oxides of coated and uncoated MA 956 before and after dynamic oxidation exposure. The oxide of the uncoated specimen with no exposure (Fig. 7a) was quite flat with some relief features. The oxide of the uncoated specimen after exposure (Fig. 7b) showed a blunting of the topography of the unexposed specimen. The surface of the coated specimen with no exposure (Fig. 7c) showed the presence of the coating that had filled most of the shallow valleys of the uncoated surface. The oxide of the coated specimen after exposure (Fig. 7d) had more texture than the coated specimen with no exposure, indicating that some oxidation of the coating occurred during exposure.

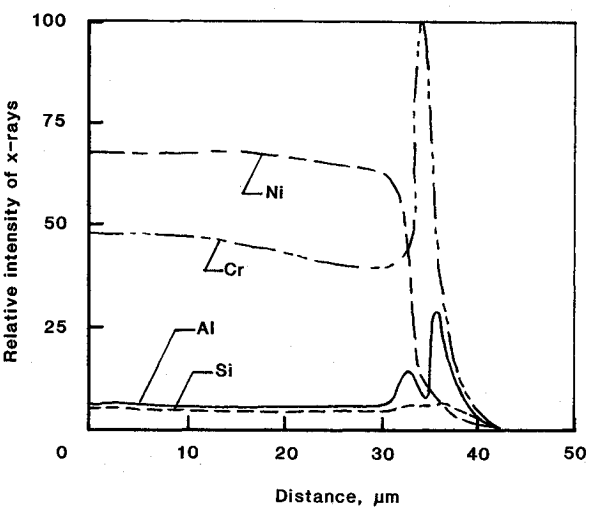

Fig. 6a Elemental profiles near surface of coated Inconel 617 specimen with no dynamic oxidation exposure.

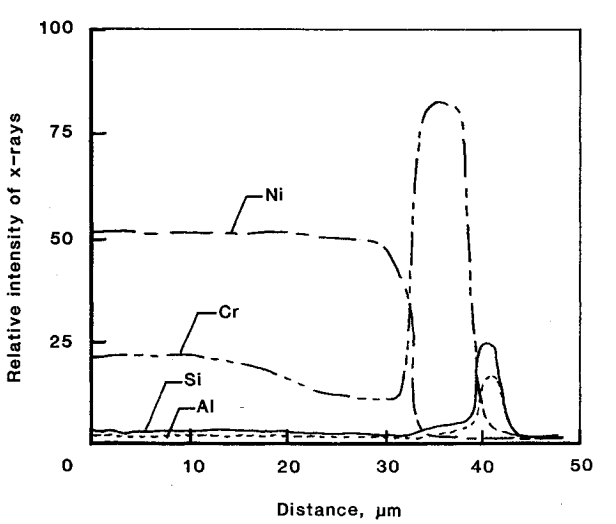

Fig. 6b Elemental profiles near surface of coated Inconel 617 specimen after 5 h dynamic oxidation at 1320 K surface temperature.

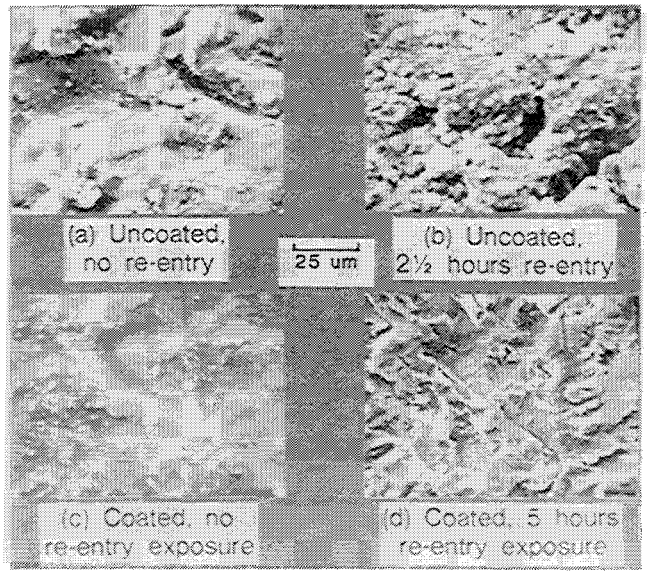

Fig. 7 SEM photographs of MA 956 specimens.

Figure 8 shows EDAX line scans of polished cross sections of coated MA 956 specimens before and after exposure to dynamic oxidation conditions. The high-intensity aluminum signal at the surface indicates the presence of the very thin layer of alumina that was formed on static oxidation of MA 956. The presence of the aluminosilicate layer at the surface is indicated by the high-intensity silicon signal. The lower relative x-ray intensity for silicon vs aluminum for the post-exposure specimen (Fig. 8b) compared to the specimen with no exposure to dynamic oxidation conditions (Fig. 8a) indicates that the coating may have experienced a loss of silicon during the test.

Radiative Properties

Table 4 presents the total normal emittance of Inconel 617 and MA 956 specimens determined from room temperature spectral reflectance data. The total emittance of coated and uncoated Inconel 617 was greater than 0.8 before and after exposure to dynamic oxidation conditions.

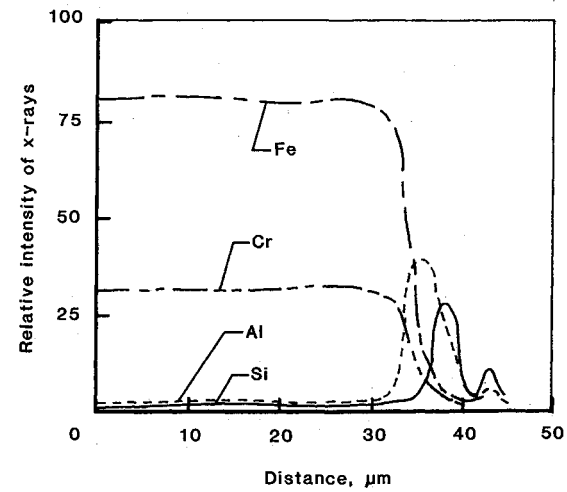

Fig. 8a Elemental profiles near surface of coated MA 956 specimen with no dynamic oxidation exposure.

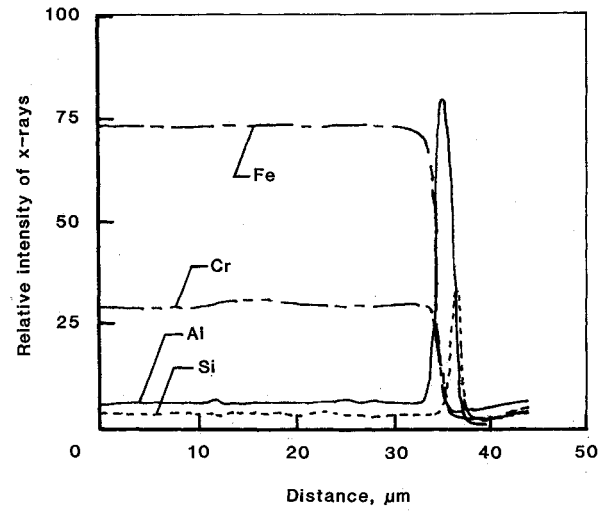

Fig. 8b Elemental profiles near surface of coated MA 956 specimen after 5 h dynamic oxidation at 1335 K surface temperature.

Table 4 Total normal emittance of superalloys[a]

Spec. no.	Surface coated	Nominal exposure temp, K	Time at temp, h	Total normal emittance at temp, K 300	810	1090	1365
[b]	No	None	0	0.68	0.80	0.83	0.84
I-201	No	1390	2.5	0.66	0.82	0.84	0.87
I-366	Yes	None	0	0.69	0.80	0.82	0.83
I-374	Yes	1340	0.5	0.77	0.83	0.83	0.84
I-369	Yes	1375	2.5	0.86	0.88	0.87	0.87
I-362	Yes	1330	5.0	0.90	0.87	0.85	0.83
I-392	Yes	1320	5.0	0.91	0.86	0.83	0.81
I-387	Yes[c]	None	0	0.80	0.85	0.86	0.86
I-376	Yes[c]	1350	5.5	0.87	0.87	0.87	0.86
I-395	Yes[d]	1350	5.5	0.90	0.88	0.87	0.86
I-377	Yes	1345	8.0	0.87	0.88	0.88	0.88
M-0	No	None	0	0.45	0.47	0.51	0.56
M-43	No	1465	1.0	0.49	0.59	0.62	0.64
M-8	Yes	1470	5.5	0.45	0.54	0.57	0.60
M-56	Yes	None	0	0.68	0.65	0.66	0.69
M-1	Yes	1350	1.0	0.61	0.56	0.60	0.60
M-4	Yes	1340	2.5	0.64	0.63	0.62	0.64
M-3	Yes	1335	5.0	0.61	0.61	0.61	0.62
M-5	Yes	1335	5.0	0.68	0.64	0.63	0.64
M-25	Yes	1380	5.5	0.64	0.62	0.61	0.63

[a]Calculated from room temperature spectral normal reflectance data. [b]Data from Ref. 3. [c]Coating thickness on 2× normal thickness for Al sublayer and for CVD layer. [d]Thickness of CVD layer is 2× normal thickness and aluminum sublayer is normal thickness.

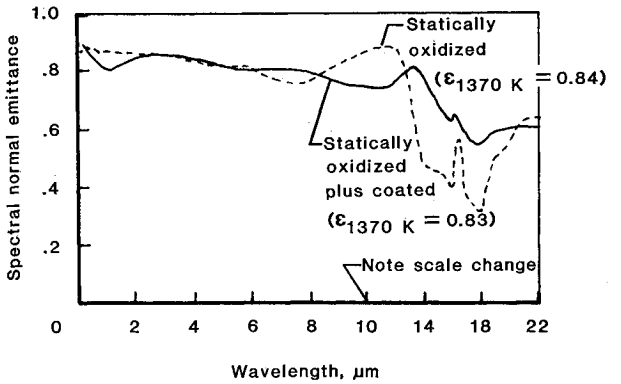

Fig. 9 Comparison of room temperature spectral emittance of coated and uncoated Inconel 617.

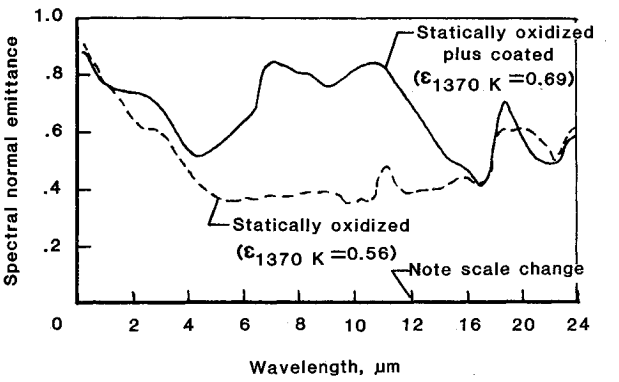

Fig. 11 Comparison of room temperature spectral emittance of coated and uncoated MA 956.

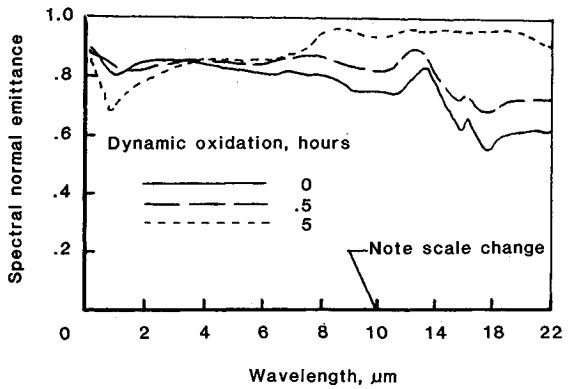

Fig. 10 Variation in room temperature spectral emittance of coated Inconel 617 with dynamic oxidation time.

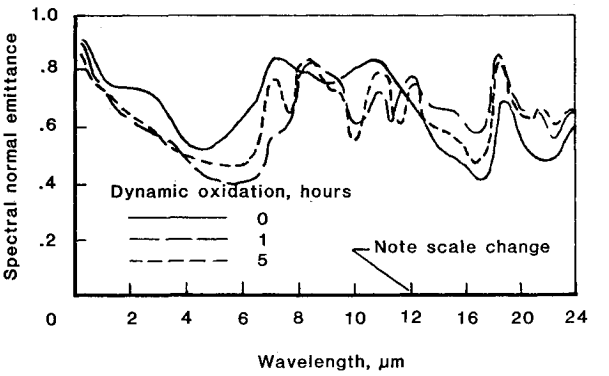

Fig. 12 Variation in spectral emittance of coated MA 956 with dynamic oxidation time.

The total normal emittance of uncoated MA 956 was less than 0.6 before exposure and greater than 0.6 after exposure. The emittance of coated MA 956 was 0.68 before exposure but it experienced a 7% reduction to about 0.62 with exposure. This value was approximately equal to the emittance of the uncoated MA 956 after exposure.

The effect of the aluminosilicate coating on the normal spectral emittance of Inconel 617 is shown in Figs. 9 and 10. Exposure to dynamic oxidation conditions resulted in significant increases in spectral emittance of coated specimens at wavelengths greater than about 8 μm. That increase in spectral emittance at longer wavelengths was indicative of a NiO-rich surface. The spectral structure observed at longer wavelengths for the statically oxidized alloys before exposure to dynamic oxidation conditions, either coated or uncoated, was the result of the Cr_2O_3 presence at the surface.[3] Oxidation of the chromia during exposure produced an excess of nickel oxide at the surface. The NiO-rich/Cr_2O_3-depleted surface layer is also evident in the EDAX data for surface analysis of post-exposure specimens (Table 5). Initially, the CR/Ni ratio of intensities was much greater than 1. After exposure to dynamic oxidation conditions the ratio was 1 or less. Nickel oxide typically has a lower emittance at short wavelengths and a higher emittance at longer wavelengths than does chromia when present in thin layers (on the order of 1-5 μm thick) over a metallic substrate.

Table 5 Summary of EDAX Cr/Ni ratios for Inconel 617

Spec. no.	Surface coated	Nominal exposure temp, K	Time at temp, h	Ratio, counts Cr to counts Ni
I-4	No	1390	1	1.6
I-201	No	1390	2.5	3.1
I-361	Yes	None	0	10.0
I-368	Yes	None	0	2.5
I-362	Yes	1330	5	0.5
I-369	Yes	1375	5	0.7

Figure 11 shows the effect of the aluminosilicate coating on the normal spectral emittance of MA 956. The coated specimen had a somewhat higher emittance than the uncoated specimen over much of the wavelength spectrum, which was the basis for higher total emittance of coated alloy compared to uncoated alloy. This increase in spectral emittance is due to the enhanced absorption coefficient of the aluminosilicate layer over the alumina layer by itself.

Figure 12 shows spectral emittance data for coated MA 956 after different dynamic oxidation exposure times. The data show an increase in spectral structure and decreases in emittance, in the 5-16-μm wavelength region with oxidation time. The spectral emittance characteristics of the coated alloy approach those of the uncoated alloy with increasing oxidation time due to the decreases in silicon relative to aluminum in the coating layer (Fig. 8). After several hours of exposure the outer layer is more aluminum-like and consequently similar to the uncoated alloy surface.

Concluding Remarks

The feasibility of using vapor-deposited coatings to increase the emittance and decrease the catalytic activity of superalloys under dynamic oxidation conditions was investigated. The effect of aluminosilicate coatings on the TPS performance characteristics of Inconel 617 and MA 956 was studied and the following results were obtained:

1) Dynamic oxidation tests of Inconel 617 and MA 956 indicated that both alloys were catalytic to the recombination

reaction of dissociated oxygen and nitrogen species that are present in Space Shuttle-like re-entry environments. Uncoated MA 956 decreased in surface catalysis ratio (the ratio of the specimen heating rate to the heating rate to a fully catalytic surface under the same condition) with exposure to dynamic oxidation conditions, reaching a stable value of about 0.8 after 5 h of exposure.

2) Vapor-deposited aluminosilicate coatings applied to Inconel 617 and MA 956 superalloys reduced the catalytic activity of both alloys. The surface catalysis ratios of coated Inconel 617 and MA 956 were about 60% of the values for the uncoated alloys.

3) The emittances of Inconel 617 and MA 956 were not significantly affected by coatings of the type and thickness investigated in this program. Coated MA 956 initially had a higher elevated-temperature total-normal emittance ($\epsilon_{TN} = 0.69$) than the uncoated alloy ($\epsilon_{TN} = 0.56$). However, the emittance of coated specimens decreased to a value of 0.63 with exposure to dynamic oxidation conditions, and the emittance of uncoated specimens increased to a value of 0.64 with exposure.

4) The vapor-deposited coating applied to Inconel 617 experienced a significant interaction with the surface oxides of the alloy on exposure to dynamic oxidation conditions. The aluminosilicate coating did not form a diffusion barrier to retard loss of Cr from the alloy. MA 956 experienced very little surface-chemistry interaction with the environment during exposure to dynamic oxidation conditions.

References

[1]Norris, B., "High Temperature [1366 K (2000 °F)] Sheet Material Selection for Use for Thermal Protection Systems," ROHR Industries Inc., Rept. No. RHR 80-017, April 1980, Chula Vista, CA.

[2]Cunnington, G.R., Fretter, E.F., and Clark, R.K., "Radiative Properties of a Nickel Based Superalloy—Inconel 617—After Simulated Earth Reentry," AIAA Paper 82-0898, June 1982.

[3]Cunnington, G.R., Funai, A.I., and McNab, T.K., "Radiative Properties of Advanced Spacecraft Heat Shield Materials," NASA CR-3740, 1983.

[4]Lowell, C. E., Deadmore, D. L., and Whittenberger, J. D., "Long-Term High-Velocity Oxidation and Hot Corrosion Testing of Several NiCrAl and FeCrAl Base Oxide Dispersion Strengthened Alloys," *Oxidation of Metals,* Vol. 17, No. 3-4, April 1982, pp. 205-21.

[5]Stewart, D.A., Rakich, J.V., and Lanfranco, M., "Catalytic Surface Effects on Space Shuttle Thermal Protection System During Earth Entry of Flights STS-2 Through STS-5," NASA CP-2283, Part 2, 1983.

[6]Foster, T., "Modifications to the NASA LaRC/Aerotherm 100-kW Arc-Heated Wind Tunnel System," NASA CR-77262, Sept. 1977.

[7]"Aerotherm Chemical Equilibrium Users Manual—ACE 1981," Acurex Corp., Rept. UM-81-11/ATD, Mountain View, CA, Aug. 1981.

[8]Schaefer, J.W., Tong, H., Clark, K.J., Suchsland, K.E., and Neuner, G.J., "Analytical and Experimental Evaluation of Flowing Air Test Conditions for Selected Metallics in a Shuttle TPS Application," NASA CR-2531, Aug. 1975.

[9]E 637-78, "Standard Method for Calculation of the Stagnation Enthalpy from Heat Transfer Theory and Experimental Measurements of Stagnation-Point Heat Transfer and Pressure," *1984 Annual Book of Standards,* Part 41, American Society for Testing Materials, 1982.

[10]Clark, R.K. and Unnam, J., "Response of Inconel 617 to Sea Salt and Re-entry Conditions," *Journal of Spacecraft and Rockets,* Vol. 23, Jan.-Feb. 1986, pp. 96-101.

[11]Tenney, D.R., Young, C.T., and Herring, H.W., "Oxidation Behavior of TD-NiCr in A Dynamic High Temperature Environment," *Metallurgical Transactions,* Vol. 5, May 1974, pp. 1001-1012.

[12]Clark, R.K., Webb, G., L., and Dries, G.A., "Mechanical/Radiative Performance of Rene' 41 in TPS Applications," *Proceedings of NASA Symposium on Recent Advances in TPS and Structures for Future Space Transportation Systems,* NASA CP-2315, 1984.